

# $\alpha$ A and $\alpha$ B peptides from human cataractous lenses show antichaperone activity and enhance aggregation of lens proteins

Om Srivastava,<sup>1</sup> Landon Wilson,<sup>3</sup> Stephen Barnes,<sup>2,3</sup> Kiran Srivastava,<sup>1</sup> Roy Joseph<sup>1</sup>

<sup>1</sup>Department of Optometry and Vision Science, University of Alabama at Birmingham, Birmingham, AL; <sup>2</sup>Department of Pharmacology and Toxicology, University of Alabama at Birmingham, Birmingham, AL; <sup>3</sup>Targeted Metabolomics and Proteomics Laboratory, University of Alabama at Birmingham, Birmingham, AL

**Purpose:** To identify and characterize properties of  $\alpha$ A- and  $\alpha$ B-crystallins' low molecular weight peptides (molecular weight [Mr] < 5 kDa) that were present in a 62-year-old human nuclear cataract, but not in normal 62-year-old human lenses.

**Methods:** Low molecular weight peptides (< 5 kDa) were isolated with a trichloroacetic acid (TCA) solubilization method from water-soluble (WS) and water-insoluble (WI) proteins of nuclear cataractous lenses of a 62-year-old donor and normal human lenses from an age-matched donor. Five commercially synthesized peptides (found only in cataractous lenses and not in normal lenses) were used to determine their chaperone and antichaperone activity and aggregation properties.

**Results:** Mass spectrometric analysis showed 28 peptides of  $\alpha$ A-crystallin and 38 peptides of  $\alpha$ B-crystallin were present in the cataractous lenses but not in the normal lenses. Two  $\alpha$ A peptides (named  $\alpha$ AP1 and  $\alpha$ AP2; both derived from the  $\alpha$ A N-terminal domain (NTD) region) and three  $\alpha$ B peptides (named  $\alpha$ BP3,  $\alpha$ BP4, and  $\alpha$ BP5, derived from the  $\alpha$ B NTD-, core domain (CD), and C-terminal extension (CTE) regions, respectively) were commercially synthesized.  $\alpha$ AP1 inhibited the chaperone activity of  $\alpha$ A- and  $\alpha$ B-crystallins, but the other four peptides ( $\alpha$ AP2,  $\alpha$ BP3,  $\alpha$ BP4, and  $\alpha$ BP5) exhibited mixed effects on chaperone activity. Upon incubation with human WS proteins and peptides *in vitro*, the  $\alpha$ BP4 peptide showed higher aggregation properties relative to the  $\alpha$ AP1 peptide. During *in vivo* experiments, the cell-penetrating polyarginine-labeled  $\alpha$ AP1 and  $\alpha$ BP4 peptides showed 57% and 85% aggregates, respectively, around the nuclei of cultured human lens epithelial cells compared to only 35% by a scrambled peptide.

**Conclusions:** The antichaperone activity of the  $\alpha$ AP1 peptide and the aggregation property of the  $\alpha$ BP4 peptide with lens proteins could play a potential role during the development of lens opacity.

Crystallins ( $\alpha$ -,  $\beta$ -, and  $\gamma$ -crystallins) constitute > 90% of the total vertebrate lens proteins. Alpha crystallin (composed of two subunits of  $\alpha$ A- and  $\alpha$ B-crystallins) exhibits chaperone function [1] to keep other crystallins soluble in their native states, and therefore, it plays a major role in maintaining lens transparency.  $\beta$ - and  $\gamma$ -crystallins are mainly structural proteins and constitute a superfamily due to their origin via gene duplication. In addition, interactions among crystallins play a major role in maintaining lens transparency [2]. However, during aging and cataract development, the native structures of crystallins and their interactions are altered. These factors, along with mutations in crystallins [3-6] and a variety of post-translational modifications (PTM), such as truncation, deamidation, oxidation, and glycation that cause aggregation of crystallins [7-17], are considered causative factors in cataract development.

Despite the low turnover of crystallins during aging [18],  $\alpha$ -,  $\beta$ -, and  $\gamma$ -crystallins show truncations during aging and cataract development, resulting in low molecular weight (LMW) polypeptides [7-12]. These LMW crystallin

polypeptides exist in water-soluble (WS) and water-insoluble (WI) protein fractions [7-12], and they are part of *in vivo* existing covalent complexes of human lenses [19,20]. Mass spectrometry studies of aged human lenses show that the majority of polypeptides are derived from  $\alpha$ A-,  $\alpha$ B-, and  $\beta$ A3/A1-crystallins. They are mostly present in the cortical region of the lens. The truncation process of crystallins begins in the outer cortex and continues to the nucleus [21]. Together, these reports suggest a potential role of crystallin fragments in the aggregation of crystallins and cataract development. However, presently, the mechanism of such a role of crystallin fragments in the aggregation process is not well understood.

Truncation of crystallins in human lenses starts in early middle age. In older human lenses, peptides with molecular weight (Mr) greater than 1,778 Da are mostly present in the WI-protein fractions, but to a lesser extent in the WS-protein fractions [22]. These LMW polypeptides are believed to compromise the structure and interaction among crystallins, facilitate protein aggregation, and reduce the chaperone activity of  $\alpha$ -crystallin [23-26]. For example, the  $\alpha$ A(66-80),  $\alpha$ B(1-18),  $\beta$ A3/A1(59-74), and  $\beta$ A3/A1(102-117) peptides increased light scattering during *in vitro* experiments and inhibited the chaperone functions of  $\alpha$ -crystallin. Furthermore, when two of the hydrophobic residues of the  $\beta$ A3/

Correspondence to: Om P. Srivastava, Department of Optometry and Vision Science, University of Alabama at Birmingham, CBSE, Rm 215, 1025 18<sup>th</sup> Street South, Birmingham, AL 35294; Phone: (205) 975-7630; FAX: (205) 996-5815, email: [srivasta@uab.edu](mailto:srivasta@uab.edu)

A1(102–117) peptide were replaced with hydrophilic residues, the substituted peptide (SDADHGERLMSFRPIC) did not show the antichaperone property [25].

Our studies and those of others [12,19,20,23–33] have indicated the involvement of crystallin fragments in aggregation and cross-linking processes in aging and cataractous human lenses. However, because of the lack of *in vivo* studies, the potential *in vivo* mechanism of lens crystallins' induced aggregation mechanism remains elusive.

Cell-penetrating peptides (CPPs), also known as protein transduction domains (PTDs), are well established for internalization with many types of cargo, such as proteins, nucleotides, siRNA nanoparticles, and peptides [34,35]. They are highly cationic and usually rich in arginine and lysine amino acids [34,36], and are able to internalize themselves into the cells by crossing the plasma membrane. These are noncovalently or covalently conjugated with the cargo to carry them inside the cells, and therefore, are an interesting tool for drug delivery [36]. Antenapedia, penetratin, HIV-tat, tranportan, pVEC, MAP, and polyarginine are well established CPPs [37]. In the present study, we used polyarginine with six arginine residues that were covalently conjugated at the N-terminal region of the desired polypeptides for cell penetration experiments.

The focus in the present study was peptides that are present in cataractous lenses but not in age-matched normal lenses. Among these peptides, five peptides of  $\alpha$ A- and  $\alpha$ B-crystallins were selected to determine their *in vitro* effects on the chaperone activity of  $\alpha$ A- and  $\alpha$ B-crystallins, and on aggregation of crystallins. In addition, the effects of selected fluorescently labeled, cell-penetrating peptides were examined on protein aggregation under *ex vivo* conditions in cultured human lens epithelial cells.

## METHODS

**Materials:** Normal human lenses with no apparent opacity were obtained from Dr. Robert Church (Emory University, Atlanta, GA), and the lenses were stored at  $-20^{\circ}\text{C}$  until used. Two normal lenses (from a 62-year-old donor and stored at  $-20^{\circ}\text{C}$  in medium 199 without phenol red) and two age-matched lenses with nuclear cataracts (recovered from a local surgeon and stored at  $-20^{\circ}\text{C}$  in medium 199 without phenol red) were separately pooled and processed as described below. The lenses were stored for about 2 years before they were used. Two normal human lenses with no opacity (from a donor 36 years of age) were also used to prepare a WS human lens lysate (WS-HLL). Prestained and unstained protein molecular weight markers were obtained from GE Biosciences (Piscataway, NJ). Unless indicated otherwise,

all other chemicals used in this study were purchased from Sigma-Millipore (St. Louis, MO) or Fisher Scientific (Atlanta, GA). Five polypeptides, two  $\alpha$ A-crystallins (named  $\alpha$ AP1 [N-terminal acetylated] and  $\alpha$ AP2) and three  $\alpha$ B-crystallins (named  $\alpha$ BP3,  $\alpha$ BP4, and  $\alpha$ BP5), were synthesized at the core facility of the Diabetic Center, Division of Gerontology, School of Medicine, University of Alabama at Birmingham. The purities of the synthetic peptides were  $> 95\%$ , as determined by their size-exclusion high-performance liquid chromatography (HPLC) analysis using a TSK G2500PW<sub>XL</sub> column (Tosoh Bioscience GmbH, Griesheim, Germany). Fluorescein isothiocyanate (FITC)-labeled  $\alpha$ AP1,  $\alpha$ BP4, and scrambled  $\alpha$ AP1 polypeptides were synthesized by Think-Peptides (Oxford, England). Insulin was obtained from Sigma-Millipore, and the Proteostat aggregate assay kit was from Enzo Life Sciences (Farmingdale, NY).

**Isolation of LMW peptides from human lenses:** The peptides ( $M_r < 5$  kDa) were isolated from WS and WI proteins of cataractous and two age-matched normal human lenses with the trichloroacetic acid (TCA) solubilization method, as previously described [38]. TCA-precipitated crystallins were removed with centrifugation as a pellet, and the soluble fractions (supernatants) were extensively dialyzed against water at  $5^{\circ}\text{C}$  to remove TCA and concentrated to dryness with lyophilization. Then, the peptide preparations were dissolved in the desired buffers as described below.

**Identification of peptides with mass spectrometry:** The TCA-solubilized peptide preparations from WS- and WI-protein fractions of the cataractous and age-matched normal human lenses were separated with sodium dodecyl sulfate-polyacrylamide gel electrophoresis (SDS-PAGE) [39] using a 15% polyacrylamide gel. The peptides with an  $M_r < 5$  kDa were excised from a gel and analyzed with mass spectrometry as described below at the Targeted Metabolomics and Proteomics Laboratory (TMPL), Department of Pharmacology and Toxicology, University of Alabama at Birmingham. Briefly, after fixing in the gel with 7% acetic acid, the excess stain was removed with an overnight wash with 100 mM ammonium bicarbonate/acetonitrile (50%/ 50% v/v). Then, disulfide bonds were reduced with 25 mM dithiothreitol at  $50^{\circ}\text{C}$  for 30 min. Next, 55 mM iodoacetamide was used in the dark for alkylation of the free thiol groups. After excess alkylating reagent was removed, gel pieces were washed with 100 mM ammonium bicarbonate for 30 min, and the gel pieces were dried in Savant SpeedVac (Thermo Fisher Scientific, Waltham, MA). Trypsin (12.5 ng/ $\mu$ l; Promega Gold Mass Spectrometry Grade) was added to each gel band and incubated overnight at  $37^{\circ}\text{C}$ . A 1:1 mixture of 1% formic acid and acetonitrile was used for peptide extraction. Extraction

was repeated, and the extracts were pooled and evaporated to dryness. The samples were resuspended in 0.1% formic acid (30  $\mu$ l) and used for the mass spectrometric analysis.

**Nano-cHiPLC–tandem mass spectrometry:** For the mass spectrometry (MS) study, a Nano cHiPLC 200  $\mu$ m  $\times$  0.5 mm trap cartridge attached to an analytical column (ChromXP C18-CL 3  $\mu$ m 120Å reverse-phase column; Eksigent, Dublin, CA) was used. A 5  $\mu$ l aliquot of each digest was loaded to the column using an Eksigent autosampler with a flow rate of 2  $\mu$ l/min. Furthermore, the cartridge was washed with 0.1% formic acid in double distilled water (ddH<sub>2</sub>O) for 4 min. The bound peptides were flushed off the cartridge and resolved on the analytical column with a 45 min linear (5% to 50%) acetonitrile gradient in 0.1% formic acid at 1,000 nl/min using an Eksigent NanoLC-1Dplus (one-dimensional nano-HPLC system). The column was washed for 10 min with 90% acetonitrile–0.1% formic acid and reequilibrated for 10 min with 5% acetonitrile–0.1% formic acid. Eluted peptides were passed through an IonSpray™ interface (voltage set at 2,300 V and a declustering potential of 80 V), and the resulting ions were analyzed on a SCIEX TripleTOF 5600 mass spectrometer (AB SCIEX, Toronto, Canada). The pressure for the Ion Spray™ and curtain gases was 10 psi and 25 psi, respectively, and the interface heater temperature was 120 °C.

To determine the 20 most intense ions for tandem mass spectrometry (MS/MS), time-of-flight survey scans of the eluted peptides from 400 to 1,250  $m/z$  of the eluted peptides were performed. To obtain the tandem mass spectra of the selected parent ions, product ion time-of-flight scans at 50 ms were performed over the range of  $m/z$  100–1500). Using Analyst software, version TF (AB SCIEX) spectra were centroided and deisotoped. To calibrate the mass accuracy of the mass spectrometer, a  $\beta$ -galactosidase trypsin digest was used. Proteins were identified from tandem mass spectrometry data using the ProteinPilot 4.5 search engine (AB SCIEX) with the *Homo sapiens* UniProt protein database. The potential candidates (proteins with at least one peptide) were selected based on a confidence score of 95% or greater, and data were exported as an Excel file. Peptides specifically detected only in the cataractous lenses were categorized in the following three groups: (1) detected in the WS-protein fraction, (2) detected only in the WI-protein fraction, and (3) detected in the WS- and WI-protein fractions.

**Selection of peptides and prediction of biochemical properties of peptides:** Five peptides, two from  $\alpha$ A-crystallin (named  $\alpha$ AP1 and  $\alpha$ AP2) and three from  $\alpha$ B-crystallin (named  $\alpha$ BP3,  $\alpha$ BP4, and  $\alpha$ BP5), were detected in the cataractous lenses but not in the age-matched normal lenses. The biochemical properties of these peptides were predicted using

**INNOVAGEN.** Furthermore, the five peptides were commercially synthesized and were characterized for their effects on the chaperone activity of  $\alpha$ A- and  $\alpha$ B-crystallins and their role in aggregation of crystallins. The  $\alpha$ AP2,  $\alpha$ BP3,  $\alpha$ AP2, and  $\alpha$ BP5 peptides were readily soluble in deionized water, whereas the  $\alpha$ AP1 and  $\alpha$ BP4 peptides were water soluble after incubation at 37 °C for 10 min.

**Antichaperone activity of the peptides:** To evaluate whether the five selected peptides exhibited chaperone activity, insulin was used as a target protein, as previously described [40,41]. The dithiothreitol (DTT)-induced aggregation of insulin (200  $\mu$ g) was performed at 37 °C for 60 min in 10 mM sodium phosphate buffer (pH 7.4, containing 100 mM sodium chloride) in a 1 ml reaction volume with and without the peptides. Varying concentrations (5, 25, 50, and 100  $\mu$ M) of each peptide were used to evaluate chaperone activity. Aggregation was monitored as turbidity at 360 nm over time (60 min) using a Shimadzu ultraviolet -visible (UV-VIS) scanning spectrophotometer (model UV2101 PC, Columbia, MD) equipped with a six-cell positioned cuvette (Shimadzu model CPS-260) and a temperature controller (Shimadzu model CPS 260).

**Effects of peptides on the chaperone activity of  $\alpha$ A- and  $\alpha$ B-crystallins:** The effect of each peptide (100  $\mu$ M) on the chaperone activity of  $\alpha$ A- and  $\alpha$ B-crystallins (100  $\mu$ g) was investigated using insulin as the target protein. Change in absorbance at 360 nm was monitored at 10-min intervals for 60 min as described above. For the experiments, recombinant  $\alpha$ A- and  $\alpha$ B-crystallins were purified from *E. coli* lysates, as previously described [40,41].

**Effects of the  $\alpha$ AP1 and  $\alpha$ BP4 peptides on the secondary structure of  $\alpha$ A- and  $\alpha$ B-crystallins:** The chaperone activity of  $\alpha$ A- and  $\alpha$ B-crystallins was inhibited by the  $\alpha$ AP1 peptide, whereas the activity was not affected by the  $\alpha$ BP4 peptide (described in the Results section). The effects of the two peptides ( $\alpha$ AP1 and  $\alpha$ BP4) on alteration in the secondary structures of  $\alpha$ A- and  $\alpha$ B-crystallins was analyzed with Circular Dichroism spectroscopy using a Jasco CD spectrometer (Easton, MD). For CD spectral analysis, 10  $\mu$ M protein ( $\alpha$ A-/ $\alpha$ B-crystallin) and 25  $\mu$ M peptide ( $\alpha$ AP1/ $\alpha$ BP4) in a 200  $\mu$ l reaction mixtures of 10 mM phosphate buffer (pH 7.4) were incubated at 37 °C for 15 min, and the secondary structures were recorded in the far-UV region (190–260 nm) using the appropriate controls (the  $\alpha$ A- or  $\alpha$ B-crystallin alone and the  $\alpha$ AP1 or  $\alpha$ BP4 peptide alone). The spectrum of the buffer alone was subtracted from each of the spectra, and the secondary structure was predicted using the Selcon 3 program (BMB).

*Aggregation of lens proteins on incubation of the  $\alpha$ API and  $\alpha$ BP4 peptides with WS-HLL:* To prepare WS-HLL, two lenses from normal humans with no opacity (36 years of age) were homogenized in 1 ml of 10 mM sodium phosphate buffer (pH 7.4, containing 100 mM sodium chloride, protease inhibitor cocktail [Millipore-Sigma]) and centrifuged at 16873  $\times g$  for 10 min at 4 °C. Supernatants were collected, and the process was repeated as described above. Both supernatants (collected after centrifugation) were pooled, designated as the human WS-HLL, and the protein concentration was determined at 280 nm. The WS protein (250  $\mu$ g) was incubated at 37 °C with 100  $\mu$ M of the selected peptides in a 200  $\mu$ l reaction mixture in 10 mM phosphate buffer (pH 7.4, containing 100 mM NaCl) for 18 h. Aggregation of the WS protein was analyzed with the Aggresome assay kit (Enzo Life Sciences) using the manufacturer's instructions with slight modifications. The Proteostat reagent was diluted 1,000X using 10 mM phosphate buffer, and 200  $\mu$ l of the diluted Proteostat reagent was added to the 200  $\mu$ l of all the WS-protein preparations that had been previously incubated for 18 h. The reaction mixture was kept in the dark for 15 min. Next, the fluorescence spectra (emission spectra between 460 and 700 nm) were recorded by excitation at 450 nm using a Shimadzu RF-5301PC spectrofluorometer with excitation and emission band passes set at 5 and 3 nm, respectively. Then, these samples were centrifuged at 16,000  $\times g$  for 10 min, and the pellets were suspended into Laemmli-SDS loading buffer and examined with SDS-PAGE using a 12% polyacrylamide gel [39]. The experiments were performed in triplicate. Additionally, human lens WS protein was incubated with 50, 100, and 200  $\mu$ M of peptides, and aggregation was determined with the aggregation assay method as described above.

*Effects of  $\alpha$ API and  $\alpha$ BP4 peptide aggregation in human lens epithelial cells:* The FITC-labeled  $\alpha$ API,  $\alpha$ BP4, and scrambled  $\alpha$ API peptides were commercially synthesized with six arginine residues at the N-terminal region of the peptides (ThinkPeptides). Human lens epithelial cells (HLECs), a kind gift from Dr. Usha Andley (Washington University, St. Louis, MO), were grown in 35 mm plates in minimum essential medium (MEM) GlutaMAX medium supplemented with 15% fetal bovine serum at 37 °C in 5% CO<sub>2</sub> until they reached > 40% confluence. Next, the cells were washed with PBS (1X; 137 mM NaCl, 2.7 mM KCl, 10 mM NaPO<sub>4</sub>, 1.8 mM KPO<sub>4</sub>, pH 7.4), and the peptides were prepared (1  $\mu$ M peptide and 3  $\mu$ l dimethyl sulfoxide (DMSO) were mixed with 1 ml serum-free medium Opti-MEM, Gibco, Thermo Fisher scientific) and added to the cells and incubated for 18 h at 37 °C in 5% CO<sub>2</sub>. Opti-MEM containing FITC-labeled peptide was removed after 18 h, and 1 ml of complete growth medium was added to the cells, followed by incubation for 6 h at 37 °C in

5% CO<sub>2</sub>. Next, the cells were washed 5X with PBS and fixed with 4% paraformaldehyde for 30 min. The cells were then washed in PBS (3X) and permeabilized with 1% Triton X-100 (Thermo Fisher scientific) and 3 mM EDTA for 30 min at 4 °C. The cells were then washed with PBS and stained with Proteostat Aggresome dye and Hoechst nuclear stain for 30 min. The cells were washed 3X with PBS and covered with coverslip. The peptides and aggregates were visualized using a Leica fluorescence microscope (Deerfield, IL) with 488 nm excitation and emission at 594 nm. In each experiment, 100 cells were manually counted using a hemocytometer to calculate the efficiency of aggregate formation in the presence of the peptides. The experiments were repeated three times.

## RESULTS

*Isolation and identification of LMW polypeptides:* LMW polypeptides ( $M_r < 5$  kDa) were isolated with a TCA-solubilization method as previously described [13]. On the SDS-PAGE of the TCA-solubilized fractions from the WS- and WI-protein fractions, peptides with an  $M_r < 5$  kDa were seen (Appendix 1). The number of peptides present in the WS- and WI-protein fractions were identified with mass spectrometry using the Protein Pilot search engine and are summarized in Table 1. These peptides showed sequence homology to  $\alpha$ -,  $\beta$ -, and  $\gamma$ -crystallins. Furthermore, in the WS-protein fraction of the normal lenses, 191  $\alpha$ A peptides and 212  $\alpha$ B peptides were identified, whereas the WS-protein fraction of the cataractous lenses showed relatively fewer peptides, that is, 72  $\alpha$ A peptides and 85  $\alpha$ B peptides (Table 1). Similarly, the WI-protein fraction of the normal lenses contained 105  $\alpha$ A peptides and 219  $\alpha$ B peptides, whereas the WI-protein fraction of the cataractous lenses contained 62  $\alpha$ A peptides and 66  $\alpha$ B peptides.

The focus of this study was to characterize those  $\alpha$ A and  $\alpha$ B peptides in WS- and WI-protein fractions that were present in cataractous lenses but not in normal lenses (Table 1). As shown in Figure 1, a total of 28  $\alpha$ A peptides (Figure 1A) and 38  $\alpha$ B peptides (Figure 1B) were identified in the cataractous lenses, and among the 28  $\alpha$ A peptides, 53% (11 peptides) were from the NTDs, and 25% and 3% were from the NTD-CD and CD-CTE regions, respectively. This suggests that predominately N-terminal domain peptides were identified in the cataractous lenses.

In the cataractous lenses, the contents of the  $\alpha$ B peptides differed from those of the  $\alpha$ A peptides. Among the  $\alpha$ B peptides, 28% were from the NTDs, 26% from the CDs, 31% from the CTE, and smaller numbers (13%) were from the CD-CTE regions. Based on the abundance of the peptides and their presence in the WS- or WI-protein fractions of the



**TABLE 1. IDENTIFIED  $\alpha$ A- AND  $\alpha$ B-PEPTIDES BY MS/MS MASS SPECTROMETRIC ANALYSIS IN TCA-SOLUBILIZED FRACTIONS FROM WS- AND WI-PROTEIN FRACTIONS OF CATARCTOUS AND AGE-MATCHED NORMAL LENSES.**

Sample (TCA-solubilized)	Number of peptides of $\alpha$ A-crystallin	Number of peptide of $\alpha$ B-crystallin
WS-Normal lenses	191	212
WI-Normal lenses	105	219
WS-cataractous lenses	72	85
WI-Cataractous lenses	62	66

cataractous lenses, the following five peptides were selected for further studies: two peptides from the NTD region of  $\alpha$ A-crystallin (named  $\alpha$ AP1 [NTD, residues 1–15] and  $\alpha$ AP2 [NTD, residues 38–50]) and three peptides from  $\alpha$ B-crystallin (named  $\alpha$ BP3 [NTD, residues 30–44],  $\alpha$ BP4 [CD, residues 130–137], and  $\alpha$ BP5 [CTE, residues 163–175]; Figure 2).

*Prediction of biochemical properties of the selected peptides:*

The biochemical properties of the five selected peptides were predicted by using an available online tool, as described in the Methods section (Table 2). Based on their amino acid sequences, four peptides were predicted to have an  $M_r$  of 1.4–1.8 kDa except the  $\alpha$ BP4 peptide with  $M_r$  of 0.8 kDa. Furthermore, the  $\alpha$ AP1 and  $\alpha$ AP2 peptides were predicted to be basic with poor water solubility, and the  $\alpha$ BP3 and  $\alpha$ BP5 peptides acidic and basic, respectively, both with good water solubility.

*Antichaperone activity of selected peptides:* Before determining the effects of the five selected peptides on the chaperone activity of  $\alpha$ A- and  $\alpha$ B-crystallins (see below), their chaperone activity at increasing concentrations (5, 25, 50, and 100  $\mu$ M) were determined by using insulin as a target protein (Figure 3). The  $\alpha$ AP1 (Figure 3A) and  $\alpha$ BP3 (Figure 3C) peptides showed increasing turbidity (aggregation) at 360 nm of insulin at their increasing concentrations, but the individual peptides alone did not show any light scattering (turbidity) by themselves at 360 nm. The  $\alpha$ AP2,  $\alpha$ BP4, and  $\alpha$ BP5 peptides also exhibited increasing turbidity of incubation with insulin up to the 50  $\mu$ M concentration (Figure 3B,D,E, respectively). However, 100  $\mu$ M of the  $\alpha$ AP2,  $\alpha$ BP4, and  $\alpha$ BP5 peptides did not significantly alter the aggregation of insulin compared to 50  $\mu$ M of peptides (data not shown). None of the peptides individually exhibited light scattering. Together, the results suggest that the five peptides showed antichaperone activity, and among them, the  $\alpha$ AP1 and  $\alpha$ BP3 peptides had the most antichaperone activity. However, the  $\alpha$ BP4 peptide was predicted to be a neutral peptide but with poor water solubility.

*Effects of selected peptides on the chaperone activity of  $\alpha$ A- and  $\alpha$ B-crystallins:* With insulin as the target protein, the chaperone activity of  $\alpha$ A- and  $\alpha$ B-crystallins was examined in the presence of 100  $\mu$ M concentrations of each of the five peptides (Figure 4). Chaperone activity of  $\alpha$ A-crystallin was inhibited in the presence of 100  $\mu$ M of the  $\alpha$ AP1 peptide (Figure 4A). However, the remaining four peptides ( $\alpha$ AP2,  $\alpha$ BP3,  $\alpha$ BP4, and  $\alpha$ BP5) did not affect the chaperone activity of  $\alpha$ A-crystallin (Figure 4B–E).

Chaperone activity of  $\alpha$ B-crystallin with insulin as the target protein in the presence of 100  $\mu$ M concentrations of individual peptides was also examined (Figure 5). Similar to the results for  $\alpha$ A-crystallin, chaperone activity of  $\alpha$ B-crystallin was maximally inhibited by the  $\alpha$ AP1 peptide (Figure 5A), whereas the  $\alpha$ BP3 and  $\alpha$ BP5 peptides also inhibited the chaperone activity of  $\alpha$ B-crystallin, but at relatively lower levels compared to the  $\alpha$ AP1 peptide. Similarly, the  $\alpha$ AP2 peptide also slightly inhibited  $\alpha$ B-crystallin chaperone activity but to a lesser level than the three other peptides (Figure 5B). However, the  $\alpha$ BP4 peptide did not show any effect on the chaperone activity of  $\alpha$ B-crystallin. Together, the results showed that among the five selected peptides, the  $\alpha$ AP1 peptide inhibited the chaperone activity of  $\alpha$ A- and  $\alpha$ B-crystallins, whereas the  $\alpha$ BP4 peptide did not show any effect on the chaperone activity of  $\alpha$ A- and  $\alpha$ B-crystallins. Furthermore, the  $\alpha$ AP2,  $\alpha$ BP3, and  $\alpha$ BP5 peptides affected only the chaperone activity of  $\alpha$ B-crystallin.

*Secondary structural changes in  $\alpha$ A- and  $\alpha$ B-crystallins in the presence of the  $\alpha$ AP1 and  $\alpha$ BP4 peptides:* The results above showed that although the  $\alpha$ AP1 peptide inhibited the chaperone activity of  $\alpha$ A- and  $\alpha$ B-crystallins, the  $\alpha$ BP4 peptide did not show any effect. Therefore, the secondary structural changes in purified recombinant  $\alpha$ A- and  $\alpha$ B-crystallins in the presence of the  $\alpha$ AP1 and  $\alpha$ BP4 peptides were examined with CD spectroscopy (Figure 6). Analysis of the far-UV CD spectra of  $\alpha$ A-crystallin showed that in the presence of 25  $\mu$ M  $\alpha$ AP1 peptide, the  $\beta$ -sheet of  $\alpha$ A-crystallin was reduced from 64.6% to 50.0%, whereas in the presence of

25  $\mu$ M  $\alpha$ BP4 peptide, the  $\beta$ -sheet of  $\alpha$ A-crystallin was 61.0% (Table 3). This suggested that the  $\alpha$ API peptide significantly changed the secondary structure of  $\alpha$ A-crystallin, whereas the  $\alpha$ BP4 peptide had a minimal effect. Similarly, the  $\alpha$ API peptide reduced the  $\beta$ -sheet of  $\alpha$ B-crystallin from 66% to

55% and increased the irregular structure from 20.9% to 42.5%. In contrast, the  $\alpha$ BP4 peptide only slightly reduced the  $\beta$ -sheet structure of the crystallin to 60.0% and increased the irregular structure only from 20.9% to 30.9%. Together, the results suggested that the  $\alpha$ API peptide significantly altered

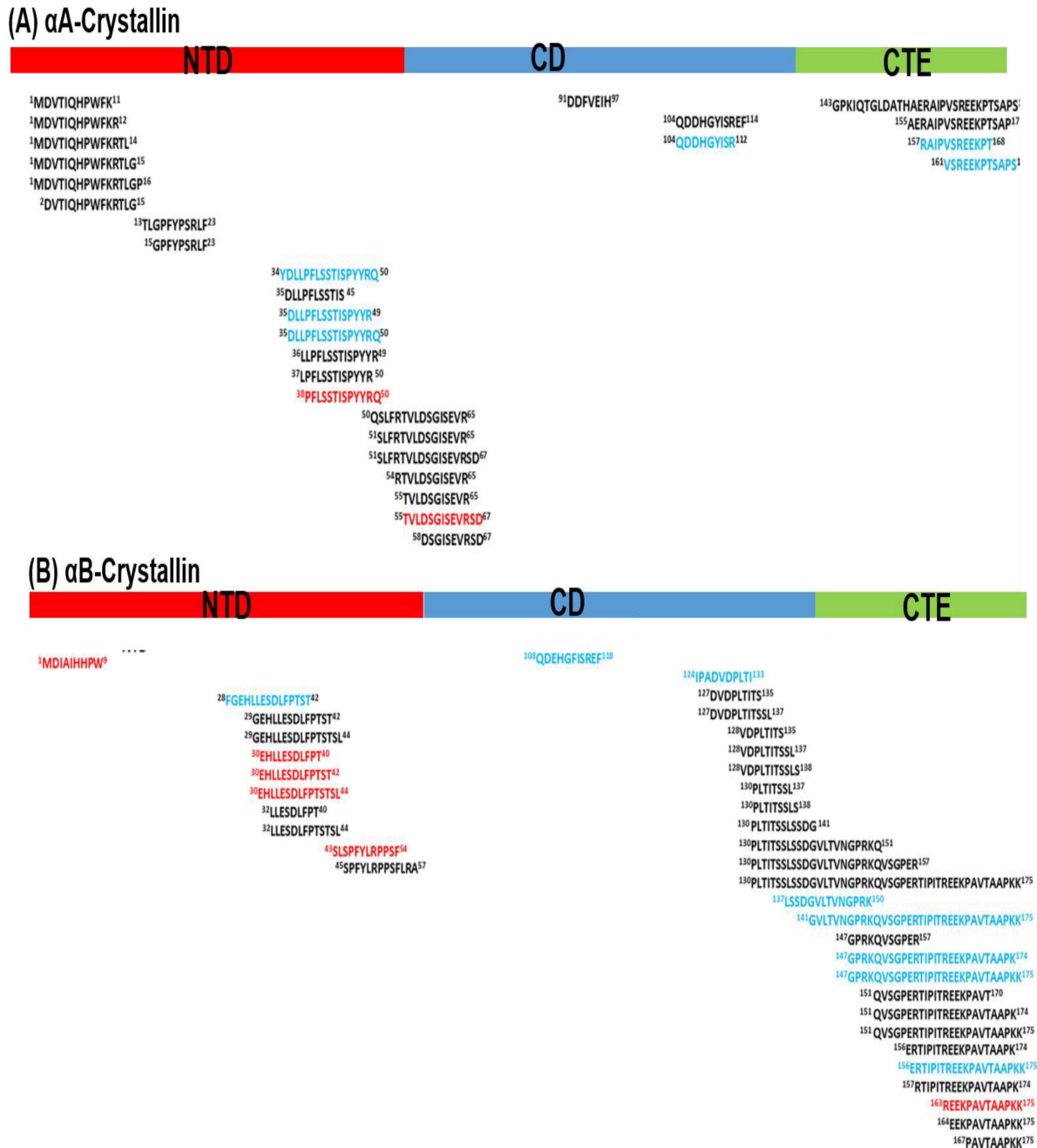


Figure 1. Endogenous LMW peptides isolated from WS- and WI-protein fractions of normal and age-matched cataractous lenses. **A:** Peptides isolated from  $\alpha$ A-crystallin. **B:** Peptides isolated from  $\alpha$ B-crystallin. Relative to normal lenses, the peptides found in cataractous lenses are as follows: Black present in WS- and WI-protein fractions in normal and cataractous lenses, blue found only in the WS-protein fraction, and red only in the WI-protein fraction.

TABLE 2. PREDICTED PROPERTIES OF FIVE SELECTED PEPTIDES OF  $\alpha$ A- AND  $\alpha$ B-CRYSTALLINS.

Peptides	Mr/pI	Charge/Attribute	Amino acid composition (%)			Water Solubility
			Acidic	Basic	Neutral	
$\alpha$ A crystallin MDVTIQHP-WFKRTL G ( $\alpha$ AP1)	1871.21/8.25	2/basic	6.67	20	26.67	Poor
PFLSSTISPYRQ ( $\alpha$ AP2)	1558.77/9.59	1/basic	0	7.69	38.46	Poor
$\alpha$ B crystallin EHLLESDF-PTSTSL ( $\alpha$ BP3)	1688.87/3.82	-2/acidic	20	6.67	33.33	Good
PLTITSSL ( $\alpha$ BP4)	830.99/6.01	0/neutral	0	0	50	Poor
REEKPAVTAAPKK ( $\alpha$ BP5)	1425.68/10.3	2/basic	15.4	30.8	7.7	Good

the secondary structures of  $\alpha$ A- and  $\alpha$ B-crystallins, but the  $\alpha$ BP4 peptide showed little effect. This could explain the loss of chaperone function of  $\alpha$ A- and  $\alpha$ B-crystallins by the  $\alpha$ AP1 peptide, but not by the  $\alpha$ BP4 peptide (Figure 5).

*Insolubilization of proteins in HLL by peptides:* The aggregation of WS proteins in HLL (at 250  $\mu$ g) was investigated in the presence of 100  $\mu$ M of the  $\alpha$ AP1-,  $\alpha$ BP4-, and scrambled  $\alpha$ AP1 peptides. Insolubilization of HLL proteins was determined with an aggregation assay using Proteostat dye, as well as with SDS-PAGE. Upon incubation, the aggregation assay showed that the WS-HLL alone formed aggregates, but the aggregation levels were increased in the presence of the  $\alpha$ AP1- and  $\alpha$ BP4 peptides (Figure 7A). The maximum levels of the aggregates were observed in the presence of the  $\alpha$ BP4 peptide, which was followed by the  $\alpha$ AP1 peptide. However, neither of these peptides showed aggregation individually. Following incubation, the aggregates were isolated with centrifugation, and the pellets were examined with SDS-PAGE. Similar to the results obtained with the aggregation assay, as shown in Figure 7A, the SDS-PAGE showed that the concentrations of WI proteins were relatively higher in the presence of the peptides compared to WS-HLL-protein

alone (Figure 7B). The results were quantified, as shown in Figure 7C. Together, these results suggested that the peptides facilitated the aggregation of human WS-HLL proteins that led to their insolubility.

To further establish whether the two peptides facilitate aggregation of WS proteins, individual peptides at 50, 100, and 200  $\mu$ M were incubated with 250  $\mu$ g WS-HLL-proteins for 18 h, and an aggregation assay was performed as described above using Proteostat dye (Figure 8). Maximum levels of aggregates were observed in the presence of 200  $\mu$ M  $\alpha$ AP1 peptide; however, the 50 and 100  $\mu$ M  $\alpha$ AP1 peptides showed almost equal levels of aggregation (Figure 8A). The levels of aggregates increased with the increasing concentrations of the  $\alpha$ BP4 peptide; the maximum aggregation level was observed at the 200  $\mu$ M concentration (Figure 8B). Together, the aggregation assay results showed that the  $\alpha$ BP4 peptide formed greater levels of aggregates at the increasing concentrations compared to the  $\alpha$ AP1 peptide.

*In vivo effects of the  $\alpha$ AP1 and  $\alpha$ BP4 peptides on HLECs:* To examine the effects of the  $\alpha$ AP1 and  $\alpha$ BP4 peptides under ex vivo conditions, HLECs in culture were treated with

### $\alpha$ A-crystallin

$\alpha$ AP1

MDVTIQHPWFKRTLGPFFPSRLFDQFFGEGLEFYDLLPFLSSTISPYRQSLFR TVLD SGISEVRS DRDKFVIFLDVKHFSP  
EDLTVKVKQDDFVEIHGKHNERQDDHGYISREFHRRYRLPSNVDQSALSCSL S ADGMLTFCGPKIQTGLDATHAERAIPVSR  
EEKPTSAPSS

$\alpha$ AP2

### $\alpha$ B-crystallin

$\alpha$ BP3

MDIAIHHPWIHRPFFPFHSPSRLFDQFFG EHLLESDFPTSTSLSPFYLRPPSFLRAPSWFDTGLSEMRLEKORFSVNLDV  
KHFSPEELKVKVLGDVIEVHGKHEERQDEHGFISREFHRRKYRIPADVDPLTITSSLS SDGVLTVNGPRKQVSGPERTIPITRE

$\alpha$ BP4

EKPAVTAAPKK

$\alpha$ BP5

Figure 2. Diagrammatic representation of the positions of the five selected peptides ( $\alpha$ AP1,  $\alpha$ AP2,  $\alpha$ BP3,  $\alpha$ BP4, and  $\alpha$ BP5) in  $\alpha$ A- and  $\alpha$ B-crystallins that were used in the study. These are identified in red, blue, and green.

1  $\mu$ M FITC-labeled peptides, as described in the Material and Methods section. Fluorescent microscopic analyses showed that the  $\alpha$ AP1 and  $\alpha$ BP4 peptides were internalized in the majority of the cells (green fluorescence) and formed intracellular aggregates (red fluorescence; Figure 9). On

quantification following manual counting of fluorescent versus non-fluorescent cells, about 57% of cells formed aggregates in the presence of the  $\alpha$ AP1 peptide, whereas a relatively greater number of cells (about 75%) formed aggregates in the presence of the  $\alpha$ BP4 peptide (Figure 9). In the

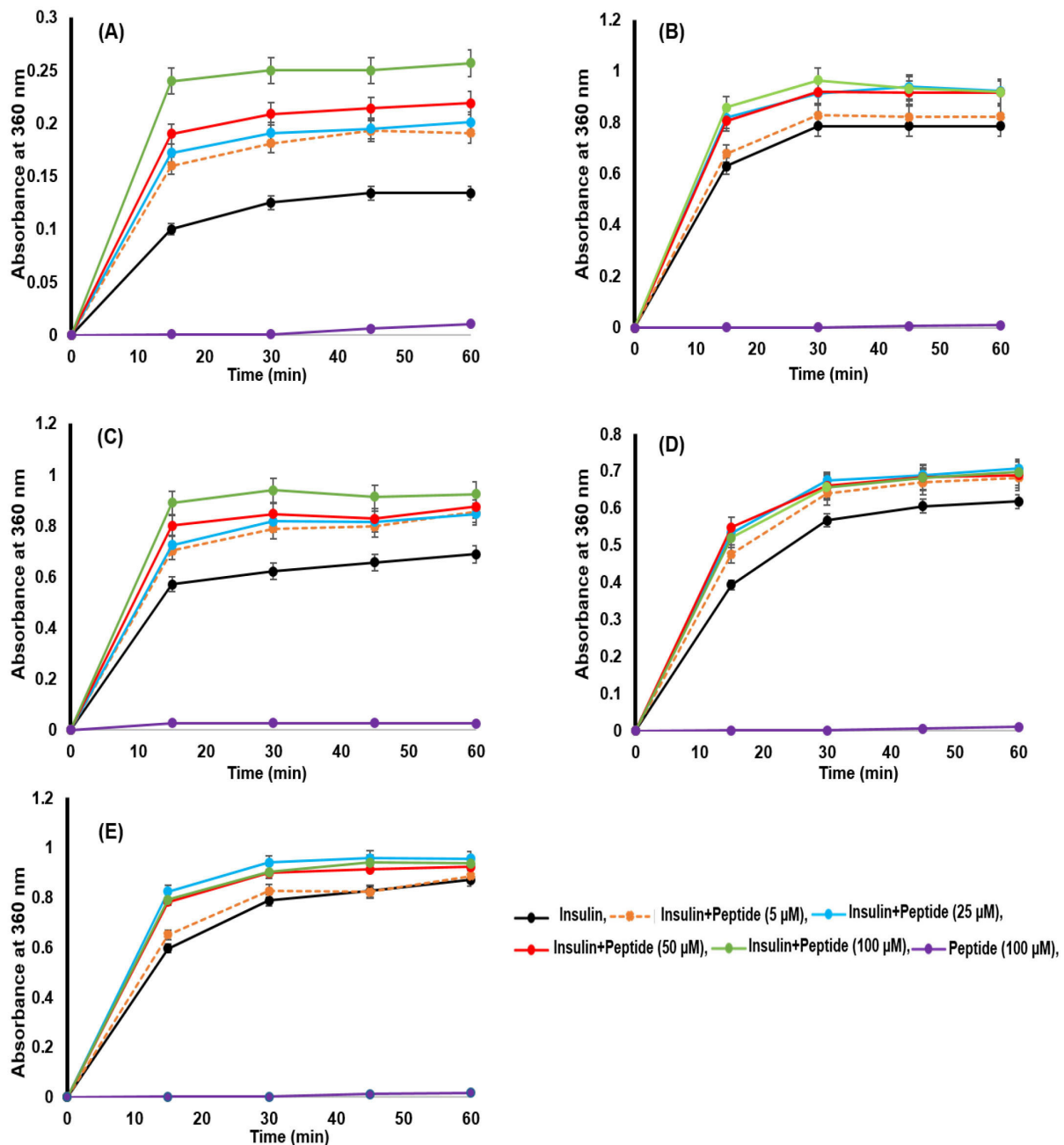


Figure 3. Determination of anti-chaperone activity of selected peptides. Antichaperone activity determination of the five selected peptides—(A)  $\alpha$ AP1, (B)  $\alpha$ AP2, (C)  $\alpha$ BP3, (D)  $\alpha$ BP4, and (E)  $\alpha$ BP5—using insulin as the target protein. The effect of various concentrations of the peptides (5, 25, 50, and 100  $\mu$ M) in aggregation of insulin (200  $\mu$ g) in the presence of dithiothreitol (DTT) at 37  $^{\circ}$ C for 60 min was determined. Absorbance at 360 nm was recorded every 15 min.



presence of either peptide, the aggregates were localized around the nuclei of the cells. Additionally, larger aggregates were observed in the presence of the  $\alpha$ BP4 peptide relative to the  $\alpha$ API1 peptide. Under similar conditions, the scrambled  $\alpha$ API1 peptide (used as a control) also formed aggregates, but

in only 35% of the cells. The results showed that the  $\alpha$ API1- and  $\alpha$ BP4 peptides facilitated aggregate formation ex vivo in lens epithelial cells, which further confirmed previous in vitro aggregation results.

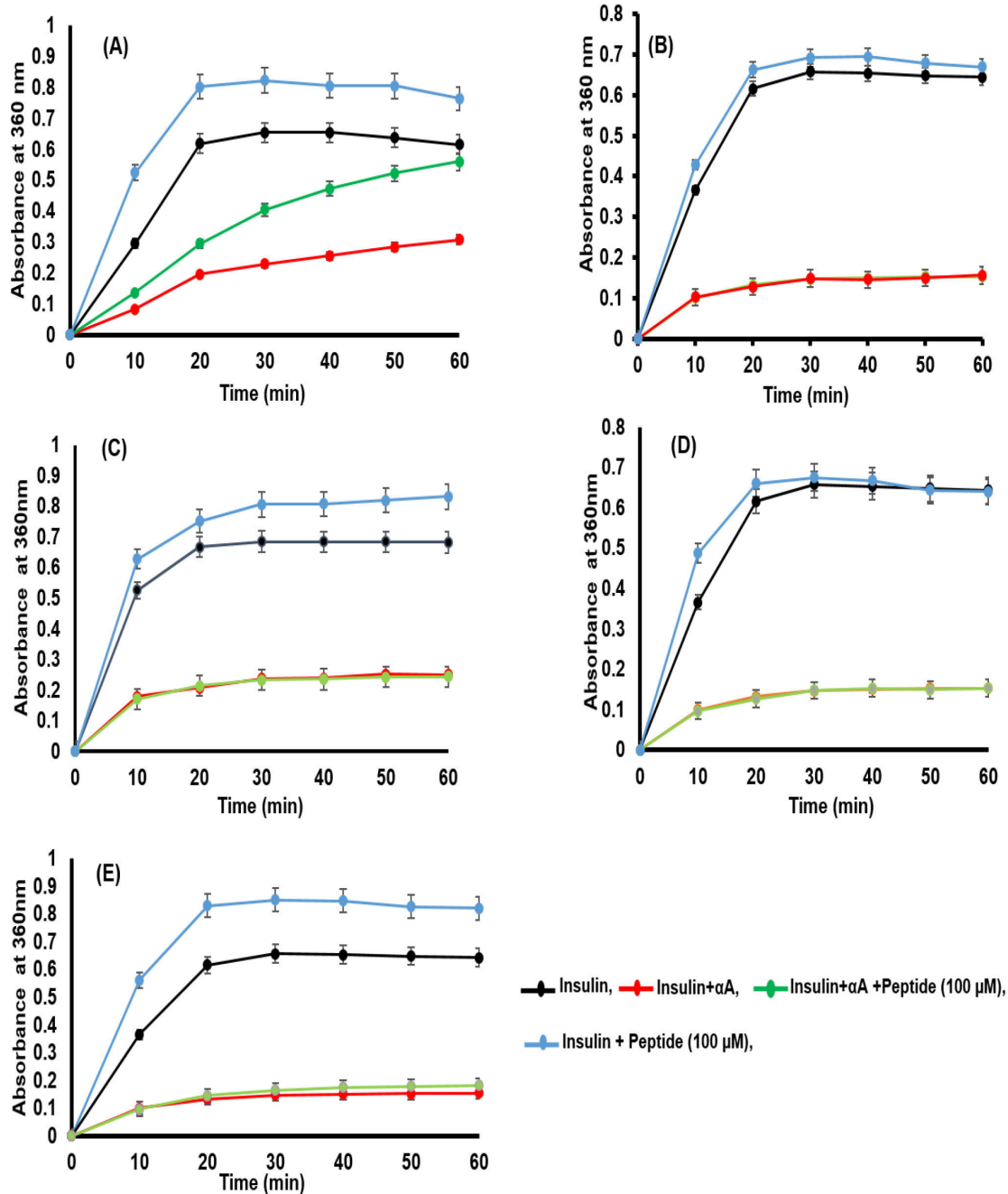


Figure 4. Effect of peptides on the chaperone activity of  $\alpha$ A-crystallin using insulin as the target protein. Effect of the five selected peptides—(A)  $\alpha$ API1, (B)  $\alpha$ AP2, (C)  $\alpha$ BP3, (D)  $\alpha$ BP4, and (E)  $\alpha$ BP5—on the chaperone activity of  $\alpha$ A-crystallin using insulin as the target protein. In the assay, 100  $\mu$ M of individual peptides with recombinant  $\alpha$ A-crystallin (100  $\mu$ g each) with insulin (200  $\mu$ g) as a target protein plus dithiothreitol (DTT) were incubated at 37 °C for 60 min. Absorbance at 360 nm was recorded every 15 min.

### DISCUSSION

The major findings of the study are as follows: (1) TCA treatment precipitated all lens proteins in the WS- and WI-protein fractions of normal and cataractous lenses, while peptides with  $M_r < 5$  kDa remained as a soluble fraction. (2) The TCA-solubilized peptides were derived from  $\alpha$ -,  $\beta$ -, and

$\gamma$ -crystallins. Among these crystallins, a greater number of  $\alpha$ A and  $\alpha$ B peptides were solubilized from the 62-year-old normal lenses and from the age-matched nuclear cataractous lenses. (3) A relatively greater number of N-terminally derived  $\alpha$ A-peptides were found in the cataractous lenses than those derived from the N-terminal region of  $\alpha$ B-crystallin.

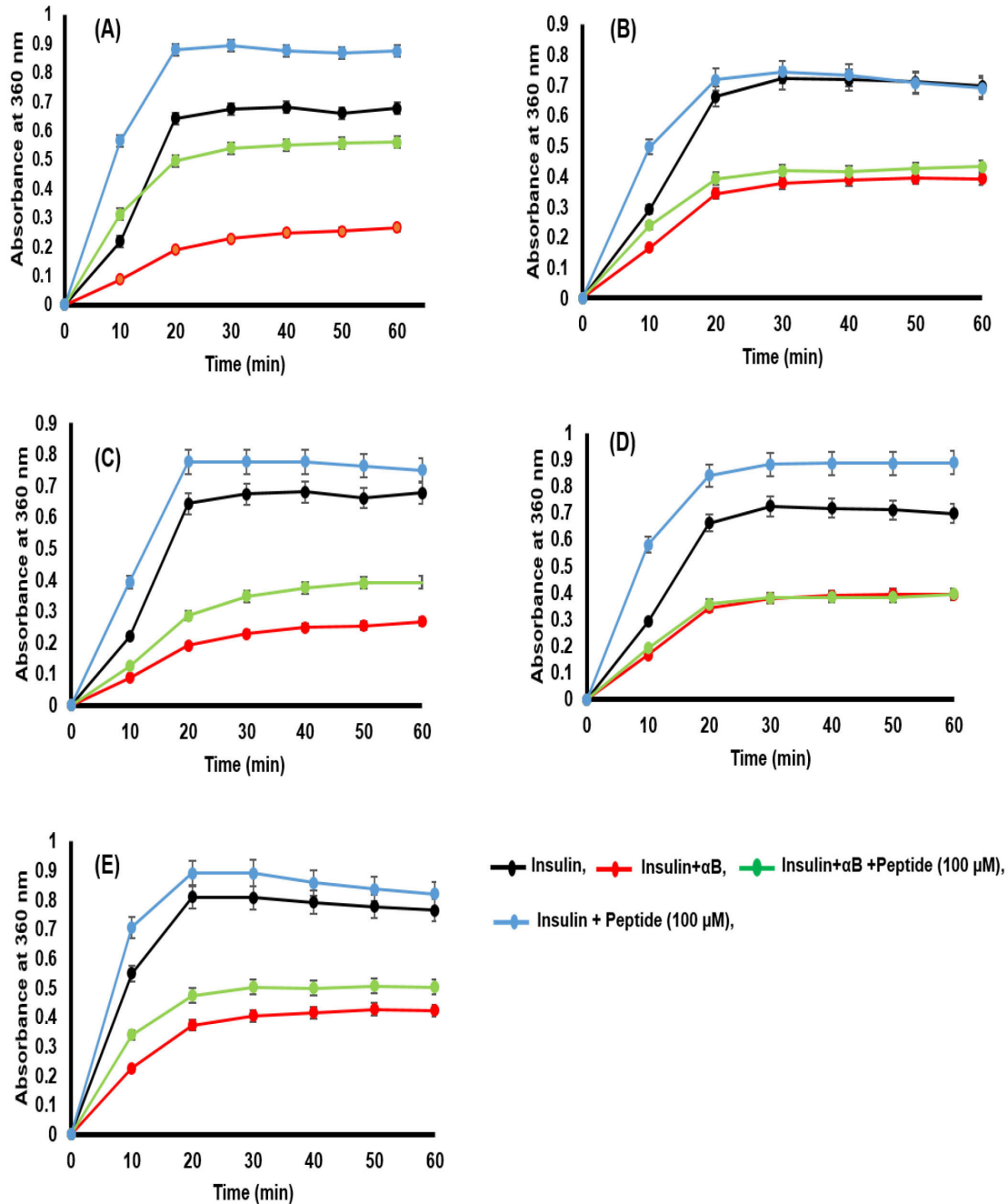


Figure 5. Effect of peptides on the chaperone activity of  $\alpha$ B-crystallin using insulin as the target protein. Effect of the five selected peptides—(A)  $\alpha$ AP1, (B)  $\alpha$ AP2, (C)  $\alpha$ BP3, (D)  $\alpha$ BP4, and (E)  $\alpha$ BP5—on the chaperone activity of  $\alpha$ B-crystallin using insulin as the target protein. The chaperone activity was determined as described in Figure 4 and the Materials and Methods section.

**TABLE 3. SECONDARY STRUCTURAL CHANGES OF  $\alpha$ A- AND  $\alpha$ B- CRYSTALLIN IN PRESENCE OF  $\alpha$ API AND  $\alpha$ BP4 DURING CD-SPECTROSCOPY.**

Sample	Helix (%)	Sheet (%)	Irregular (%)
$\alpha$ A	7.3	64.6	27.7
$\alpha$ A+ $\alpha$ API	8	50.6	37
$\alpha$ A+ $\alpha$ BP4	1.4	61.1	20
$\alpha$ B	7.5	66.8	20.9
$\alpha$ B+ $\alpha$ API	6.3	55.6	42.5
$\alpha$ B+ $\alpha$ BP4	6.2	59.8	30.9
$\alpha$ API	1.41	45.3	37.7
$\alpha$ BP4	2.3	50.3	35.4

The TCA-solubilized fractions contained relatively fewer peptides derived from the CD and C-terminal region of the  $\alpha$ A- and  $\alpha$ B-crystallins. (4) Based on the abundance of the peptides, five peptides—two  $\alpha$ A peptides ( $\alpha$ API(1–15) and  $\alpha$ AP2(38–50)) and three  $\alpha$ B peptides ( $\alpha$ BP3(30–44),  $\alpha$ BP4(130–137), and  $\alpha$ BP5 (163–175))—were commercially synthesized. Among the five peptides, the maximum anti-chaperone and aggregation properties were associated with the  $\alpha$ API peptide and the  $\alpha$ BP4 peptide, respectively.

Although long-lived crystallins have almost no turnover [18], cleavages in lens crystallins occurs during aging and cataract formation [28–30]. Whether the cleavages of these crystallins occur due to enzymatic or non-enzymatic mechanisms is not well understood [42–44]. The clearance of cleaved crystallin fragments is believed to occur via the

proteasome or ubiquitin system [43]. However, the systems operate only in lens epithelial cells and cells in the outer cortical region because of the loss of organelles in the inner cortical and nuclear regions. It has also been shown that the cleavages in crystallins occur at serine residues as a preferred site with involvement of either a yet unidentified serine-type protease or an unidentified mechanism [22,44,45]. However, despite several yet unknown factors that generate crystallin fragments or small peptides in vertebrate lenses, their accumulation during aging and cataract development is well established [8,10,11,24,25,39].

The focus of the present study was to determine the potential roles of the five selected peptides described above on chaperone activity of  $\alpha$ A- and  $\alpha$ B-crystallins and their aggregation properties. Although previous studies have not

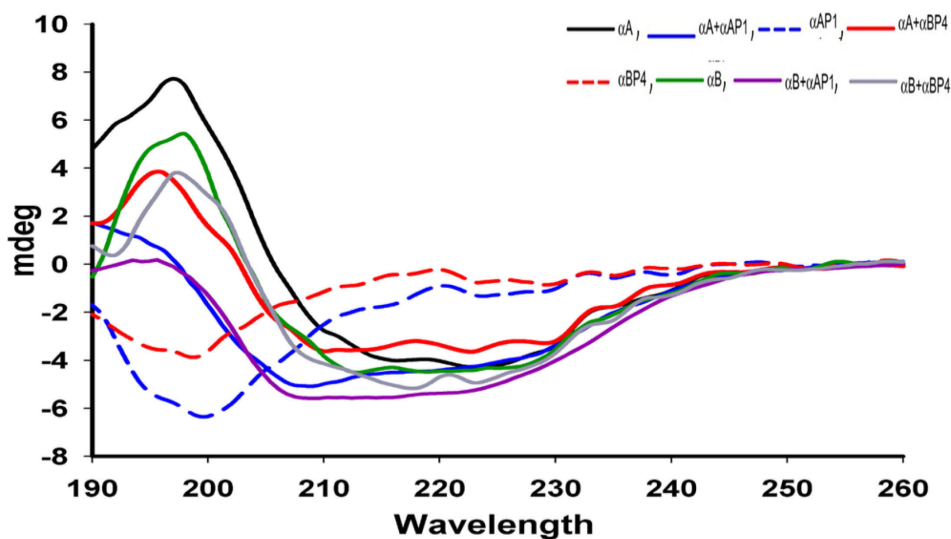


Figure 6. Determination of the effects of the  $\alpha$ API and  $\alpha$ BP4 peptides on the secondary structure of  $\alpha$ A- and  $\alpha$ B-crystallins with CD spectroscopy. For circular dichroism (CD) spectral analysis, 10  $\mu$ M protein ( $\alpha$ A- or  $\alpha$ B-crystallin) and 25  $\mu$ M peptide ( $\alpha$ API or  $\alpha$ BP4) in 200  $\mu$ l reaction mixtures of 10 mM phosphate buffer (pH 7.4) were incubated at 37  $^{\circ}$ C for 15 min, and the secondary structures were recorded in the far-ultraviolet (UV) region (190–260 nm) using a Jasco CD spectrometer and appropriate controls ( $\alpha$ A- or  $\alpha$ B-crystallin alone and the  $\alpha$ API or  $\alpha$ BP4 peptide

alone). The spectrum of the buffer alone was subtracted from each spectrum, and the secondary structure was predicted using the Selcon 3 program.

shown that the five peptides are present in human cataractous lenses relative to age-matched normal lenses, specific cleavages in the regions of crystallins that could produce the peptides have been reported. (1) Similar to the  $\alpha$ A1(1–15) peptide,  $\alpha$ A(2–12) peptide has been detected [46]. (2) Similar to the  $\alpha$ AP2(38–50) peptide, an  $\alpha$ A(37–49) peptide was detected [45]. (3) Similar to the  $\alpha$ BP3(30–44) peptide, an  $\alpha$ B(28–39) peptide was also detected [45,47]. (4) Similar to the  $\alpha$ BP4 peptide, an  $\alpha$ B(130–137) peptide was seen [47]. (5)

Similar to the  $\alpha$ BP5 (163–175) peptide,  $\alpha$ B peptides, with residue 155–175, 157–155, and 160–175, were also detected [45].

Previous studies have implicated crystallin fragments in the development of lens opacity because they exhibited inhibition of chaperone activity of  $\alpha$ -crystallin and enhanced aggregation of lens proteins [25,26].  $\alpha$ A- and  $\alpha$ B-crystallins mediated the protection of lens cells against heat and oxidative stress-induced cell death [45]. Similarly, intraperitoneal

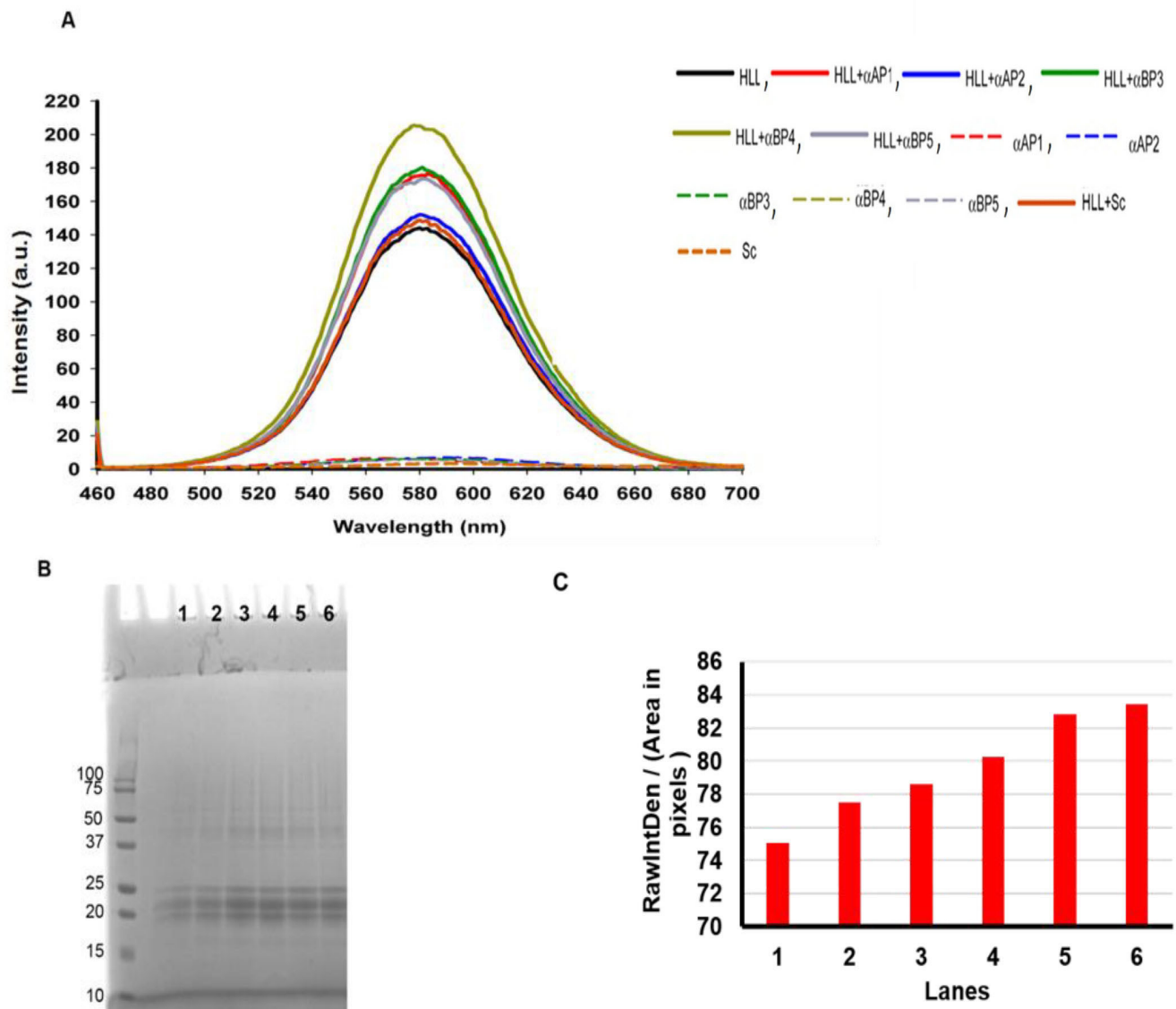


Figure 7. Aggregation of lens proteins on incubation  $\alpha$ AP1 and  $\alpha$ BP4 peptides with WS-HLL. The water soluble (WS) protein (250  $\mu$ g) was incubated at 37 °C with 100  $\mu$ M of the selected peptides in a 200  $\mu$ l reaction mixture in 10 mM phosphate buffer (pH 7.4, containing 100 mM NaCl) for 18 h. Aggregation of the WS protein was analyzed with the Aggresome assay kit (Enzo Life Sciences) using the manufacturer's instructions as described in the Materials and Methods section. Experiments were performed in triplicate, but the results of only one set are presented.



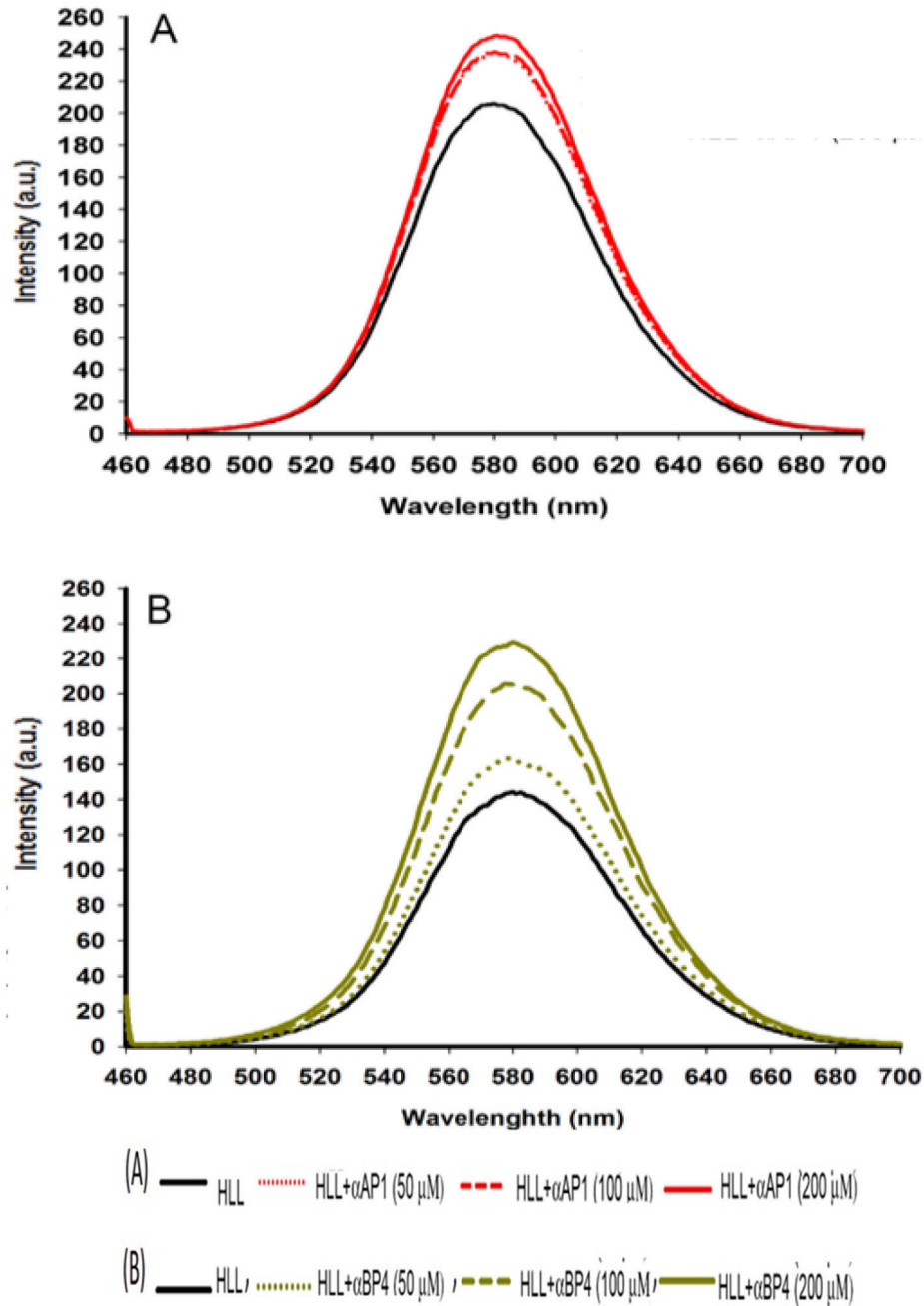


Figure 8. Emission spectra of HLL (250 µg) in the presence of 50, 100, and 200 µM peptides after 18 h incubation at 37 °C. A: The αAPI peptide. B: The αBP4 peptide.

injection of the minichaperones of the αA peptide (<sub>70</sub>KFVI-FLDVKHFSPEDLTVK<sub>88</sub>) and the αB peptide (<sub>73</sub>DRFSVN-LDVKHFSPPEELKVK<sub>92</sub>) inhibited cataract development in selenite-treated rats, which was accompanied by inhibition of oxidative stress, protein insolubilization, and induction of caspase activity [47]. Although the independent existence of these minichaperones within the lens has not been

demonstrated, if they exist, these peptides would be beneficial for lens cell survival.

In this study, a higher number of peptides (a total of 38) were identified from αB-crystallin compared to 28 peptides from αA-crystallin (Figure 1) that were present in cataractous lenses. This suggested relatively greater susceptibility to cleavage of αB-crystallin compared to αA-crystallin in

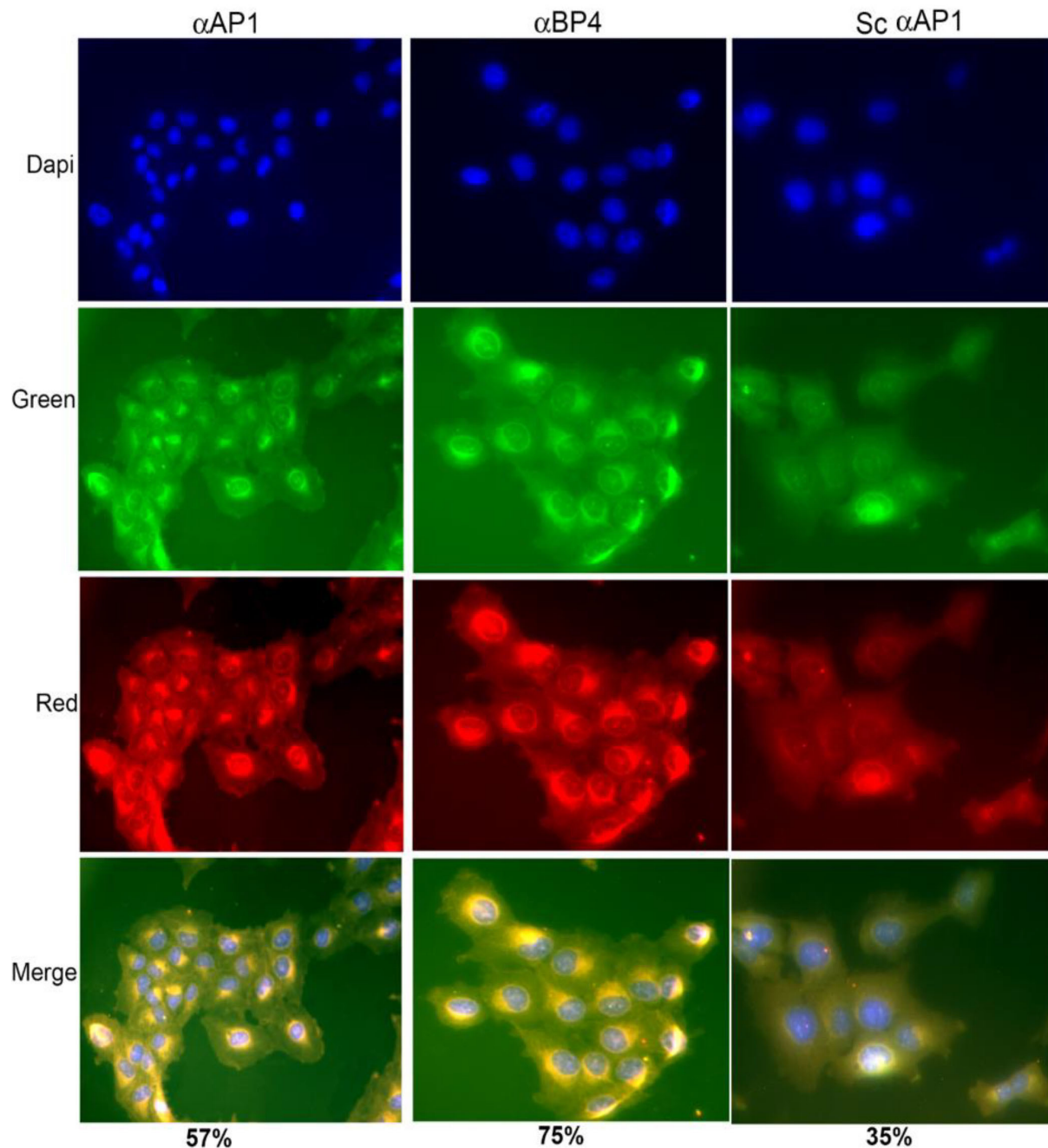


Figure 9. Aggregate formation by internalized FITC-labeled  $\alpha$ AP1,  $\alpha$ BP4, and scrambled peptides in human lens epithelial cells (HLEB3) in culture. The cells were permeabilized and then treated with Proteostat Aggresome dye. In the cells, individual peptides alone showed green fluorescence, and red fluorescence by aggregated peptides reactive to Proteostat Aggresome dye, along with cellular nuclei (stained blue with Hoechst stain). The merged image shows the overlay of the green and red fluorescence of cells. Each experiment was performed in triplicate, and 100 cells with either red or green fluorescence or both were manually counted with a hemocytometer using a Leica fluorescent microscope.

cataractous lenses, as was reported in our previous study [29]. The majority of the  $\alpha$ A peptides (53%) and  $\alpha$ B peptides (28%) were generated from the N-terminal region and fewer from the CD and CTE regions, which was also reported by us [22,24]. Only three peptides and 13 peptides were observed from the C-termini of  $\alpha$ A- and  $\alpha$ B-crystallins, respectively, only in cataractous lenses. This result differed from previous studies by Kumar et al. [25], in which they did not find any peptides from the CTE region of  $\alpha$ -crystallin, and that of Su et al. [22], who reported only a few peptides from the CTE region of  $\alpha$ A- and  $\alpha$ B-crystallins. Similar to other studies, only a few peptides from  $\beta$ - and  $\gamma$ -crystallins were also recovered in the TCA-soluble fractions (data not presented). Although peptides with N-termini from  $\alpha$ A- and  $\alpha$ B-crystallins were recovered in greater abundance, previous reports have suggested a greater susceptibility of amino acids from the CTE region to proteolytic cleavage [43,44]. A few peptides were reported to increase the surface hydrophobicity of  $\alpha$ -crystallin, which might expose the NTD region of  $\alpha$ -crystallin and make the region unstable and cleavage susceptible [27]. Su et al. analyzed NTD peptides and suggested that cleavage targeting serine residues is a non-enzymatic process, such as internal splicing and spontaneous peptide bond cleavage [22]. However, this study also suggested that a trypsin-like proteolytic cleavage might also be responsible [22].

All five selected peptides (two from the NTD of  $\alpha$ A-crystallin and three from  $\alpha$ B-crystallin [one peptide from each NTD, CD, and CTE]) exhibited light scattering with insulin as the target protein. Similarly, the  $\alpha$ A(66–80),  $\alpha$ B(1–18), and  $\beta$ A3/A1(59–74) peptides were also reported to increase light scattering of  $\alpha$ -crystallin with alcohol dehydrogenase as the target protein [24,25,27,48]. In these studies, most of the peptides were hydrophobic, and possibly their interactions with hydrophobic residues of the target protein facilitated aggregation. Among the five peptides, the  $\alpha$ API peptide maximally inhibited the chaperone function of  $\alpha$ A- and  $\alpha$ B-crystallins, whereas the  $\alpha$ BP4 peptide did not show any effect. The three remaining peptides ( $\alpha$ AP2,  $\alpha$ BP3, and  $\alpha$ BP5) slightly inhibited the chaperone activity of  $\alpha$ B-crystallin; however, they did not show any effect on the chaperone function of  $\alpha$ A-crystallin. The CD spectra showed a significant alteration in the secondary structures of  $\alpha$ A- and  $\alpha$ B-crystallins in the presence of the  $\alpha$ API peptide, but only a slight alteration in the presence of the  $\alpha$ BP4 peptide (Figure 6), suggesting that the chaperone activities of  $\alpha$ A- and  $\alpha$ B-crystallins were affected due to their secondary structural changes in the presence of the  $\alpha$ API peptide. These results are similar to the earlier reported loss of the chaperone activity

of crystallins by the peptides  $\alpha$ A(66–80),  $\alpha$ B(1–18), and  $\beta$ A3/A1(59–74) [24-26,48].

Presently, the mechanism of the antichaperone activity of crystallin peptides is not well understood. The amyloid fibrils are speculated to play a major role in the chaperone and antichaperone mechanisms of a protein. Amyloids are self-assembled, highly ordered linear aggregates of a soluble protein or peptide. One key factor that describes whether an amyloid structure of a protein or peptide would display chaperone-like or antichaperone activity is its electrostatic interactions with a presented substrate [49]. If the surface charges of amyloid fibrils on binding to a substrate are cancelled, its colloidal stability is reduced, and it facilitates protein aggregation. For example, a recent study showed that A $\beta$ (25–35) amyloid contains a net positive charge at a neutral pH and on interaction with a negatively charged acidic protein by electrostatic interaction facilitated aggregation [49]. This suggested that the amyloid fibrils' property of chaperone-like or antichaperone activity is based on their colloidal stability following electrostatic interaction, with a substrate [49]. Presently, we do not know whether the  $\alpha$ API peptide forms amyloid fibrils, and an investigation is planned as future research.

The present study showed that although the  $\alpha$ API and  $\alpha$ BP4 peptides caused aggregation of proteins in the WS-HLL human lens homogenate (Figure 7), there was greater aggregation by the  $\alpha$ BP4 peptide relative to the  $\alpha$ API peptide. The increasing peptide levels occur in human lens WS-HLL with age or during cataract development, and these peptides may play a role in the insolubilization of the WS proteins. A recent study showed that  $\alpha$ A(66–80) peptide formed aggregates, and the resulting peptide- $\alpha$ -crystallin aggregates were resistant to dissociation with high ionic strength, except in high dissociating agents such as guanidium hydrochloride and urea [27]. The study showed that the peptide formed a hydrophobically driven stable complex with  $\alpha$ -crystallin, which reduced the solubility of the latter. Therefore, the crystallins' peptides could play a potential role in the insolubilization of proteins during cataract development [24-26,45].

The present study also showed that 1  $\mu$ M  $\alpha$ API and  $\alpha$ BP4 peptides formed aggregates in HLECs under ex vivo conditions. The  $\alpha$ API,  $\alpha$ BP4, and scrambled  $\alpha$ API peptides were covalently conjugated with FITC and six arginine residues at their N-termini, as the use of polyarginine is a more efficient method among cell-penetrating homopolypeptides [34-37]. They are highly cationic and therefore easily cross the cell membrane. The  $\alpha$ BP4 peptide showed maximal protein aggregates (about 75%) in cells relative to 57% cells by the  $\alpha$ API peptide, but only about 35% cells by the scrambled  $\alpha$ API

peptide (Figure 9). The  $\alpha$ BP4 peptide also formed bigger aggregates than the  $\alpha$ API peptide, and they were present around the nucleus. We do not know whether the neutral and hydrophobic nature of the  $\alpha$ BP4 and  $\alpha$ API peptides, respectively, are responsible for the difference in their in vivo aggregation properties. A previous study showed that the  $\alpha$ A(66–80) peptide interacted with soluble  $\alpha$ -crystallin and induced its aggregation and precipitation, and it was believed that the  $\alpha$ A(66–80) peptide formed a hydrophobically driven, stable complex with  $\alpha$ -crystallin and reduced its solubility.

In summary, we identified peptides from cataractous lens, which showed antichaperone activity and facilitated aggregation of proteins in ex vivo and in vitro conditions. In the future, we plan to investigate the potential mechanism of  $\alpha$ API peptide-induced antichaperone activity and  $\alpha$ BP4-induced aggregation of lens crystallins.

#### APPENDIX 1. SDS-PAGE ANALYSIS OF LMW POLYPEPTIDES ISOLATED FROM WS- AND WI-PROTEIN FRACTIONS OF 62-YEAR OLD NORMAL AND AGE-MATCHED CATARACTOUS LENSES.

To access the data, click or select the words “Appendix 1.” Lanes (1) and (2) show TCA-solubilized proteins from WS-protein fraction, and WI-protein fractions of normal lenses, respectively. Lanes (3) and (4) show TCA-solubilized proteins from WS-protein fraction, and WI-protein fractions of cataractous lenses.

#### ACKNOWLEDGMENTS

The work presented is supported by grants from NIH: EY-06400 (OS) and P30EY003039. The mass spectrometer was purchased from a NIH Shared Instrumentation Award (S10 RR027822 to SB).

#### REFERENCES

- Horwitz J. Alpha-crystallin can function as a molecular chaperone. *Proc Natl Acad Sci USA* 1992; 89:10449-53. [PMID: 1438232].
- Takemoto L, Sorensen CM. Protein-protein interactions and lens transparency. *Exp Eye Res* 2008; 87:496-501. [PMID: 18835387].
- Chen J, Ma Z, Jiao X, Fariss R, Kantorow WL, Kantorow M, Pras E, Frydman M, Pras E, Riazuddin S, Riazuddin SA, Hejtmancik JF. Mutations in FYCO1 cause autosomal-recessive congenital cataracts. *Am J Hum Genet* 2011; 88:827-638. [PMID: 21636066].
- Zhang W, Cai H-C, Li F-F, Xi Y-B, Ma X, Yan Y-B. The congenital cataract-linked G61C mutation destabilizes  $\gamma$ D-crystallin and promotes non-native aggregation. *PLoS One* 2011; 6:e20564. [PMID: 21655238].
- Kong XD, Liu N, Shi HR, Dong JM, Zhao ZH, Liu J, Li-Ling J, Yang YX. A novel 3-base pair deletion of the *CRYAA* gene identified in a large Chinese pedigree featuring autosomal dominant congenital perinuclear cataract. *Genet Mol Res* 2015; 14:426-326. [PMID: 25729975].
- Ma Z, Yao W, Chan CC, Kannabiran C, Wawrousek E, Hejtmancik JF. Human  $\beta$ A3/A1-crystallin splicing mutation causes cataracts by activating the unfolded protein response and inducing apoptosis in differentiating lens fiber cells. *Biochim Biophys Acta* 2016; 1862:1214-27. [PMID: 26851658].
- Hanson SR, Hasan A, Smith DL, Smith JB. The major in vivo modifications of the human water-insoluble lens crystallins are disulfide bonds, deamidation, methionine oxidation and backbone cleavage. *Exp Eye Res* 2000; 71:195-207. [PMID: 10930324].
- Harrington V, McCall S, Huynh S, Srivastava K, Srivastava OP. Crystallins in water soluble-high molecular weight protein fractions and water insoluble protein fractions in aging and cataractous human lenses. *Mol Vis* 2004; 10:476-89. [PMID: 15303090].
- Ma ZX, Hanson SRA, Lampi KJ, David LL, Smith D, Smith JB. Age-related changes in human lens crystallins identified by HPLC and mass spectrometry. *Exp Eye Res* 1998; 67:21-30. [PMID: 9702175].
- Lampi KJ, Ma Z, Hanson SRA, Azuma M, Shih M, Shearer TR, Smith DL, Smith JB, David LL. Age-related changes in human lens crystallins identified by two-dimensional gel electrophoresis. *Exp Eye Res* 1998; 67:31-43. [PMID: 9702176].
- Santhoshkumar P, Udupa P, Murugesan R, Sharma KK. Significance of interactions of low molecular weight crystallin fragments in lens aging and cataract formation. *J Biol Chem* 2008; 283:8477-85. [PMID: 18227073].
- Srivastava OP, Srivastava K, Chaves JM, Gill AK. Post-translationally modified human lens crystallin fragments show aggregation in vitro. *Biochem Biophys Rep* 2017; 10:94-131. [PMID: 28955739].
- Srivastava OP, Srivastava K. Existence of deamidated  $\alpha$ B-crystallin fragments in normal and cataractous human lenses. *Mol Vis* 2003; 9:110-8. [PMID: 12707643].
- Wilmarth PA, Tanner S, Dasari S, Nagalla SR, Riviere MA, Bafna V, Pevzner PA, David LL. Age-related changes in human crystallins determined from comparative analysis of post-translational modifications in young and aged lens: Does deamidation contribute to crystallin insolubility? *J Proteome Res* 2006; 5:2554-66. [PMID: 17022627].
- Ortwerth BJ, Slight SH, Prabhakaram M, Sun Y, Smith JB. Site-specific glycation of lens crystallins by ascorbic acid. *Biochim Biophys Acta* 1992; 1117:207-15. [PMID: 1525182].
- Nagaraj RH, Monnier VM. Isolation and characterization of a blue fluorophore from human eye lens crystallins: in vitro



- formation from Maillard reaction with ascorbate and ribose. *Biochim Biophys Acta* 1992; 1116:34-42. [PMID: 1540622].
17. Fan X, Zhang J, Theves M, Strauch C, Nemet I, Liu X, Qian J, Giblin FJ, Monnier VM. Mechanism of lysine oxidation in human lens crystallins during aging and in diabetes. *J Biol Chem* 2009; 284:34618-27. [PMID: 19854833].
  18. Stewart DN, Lango J, Nambiar KP, Falso MJS, FitzGerald PG, Rocke DM, Hammock BD, Buchholz BA. Carbon turnover in the water-soluble protein of the adult human lens. *Mol Vis* 2013; 19:463-75. [PMID: 23441119].
  19. Srivastava K, Chaves JM, Srivastava OP, Kirk M. Multi-crystallin complexes exist in the water-soluble high molecular weight protein fractions of aging normal and cataractous human lenses. *Exp Eye Res* 2008; 87:356-66. [PMID: 18662688].
  20. Srivastava OP, Kirk MC, Srivastava K. Characterization of covalent multimers of crystallins in aging human lenses. *J Biol Chem* 2004; 279:10901-9. [PMID: 14623886].
  21. Asomugha CO, Gupta R, Srivastava OP. Identification of crystallin modifications in the human lens cortex and nucleus using laser capture microdissection and CyDye labeling. *Mol Vis* 2010; 16:476-94. [PMID: 20352024].
  22. Su SP, Song X, Xavier D, Aquilina JA. Age-related cleavages of crystallins in human lens cortical fiber cells generate a plethora of endogenous peptides and high molecular weight complexes. *Proteins* 2015; 83:1878-86. [PMID: 26238763].
  23. Sharma KK, Kumar RS, Kumar GS, Quinn PT. Synthesis and characterization of a peptide identified as a functional element in alphaA-crystallin. *J Biol Chem* 2000; 275:3767-71. [PMID: 10660525].
  24. Santhoshkumar P, Udupa P, Murugesan R, Sharma KK. Significance of interactions of low molecular weight crystallin fragments in lens aging and cataract formation. *J Biol Chem* 2008; 283:8477-85. [PMID: 18227073].
  25. Santhoshkumar P, Raju M, Sharma KK. alphaA-crystallin peptide SDRDKFVIFLDVKHF accumulating in aging lens impairs the function of alpha-crystallin and induces lens protein aggregation. *PLoS One* 2011; 6:e19291. [PMID: 21552534].
  26. Senthilkumar R, Chaerkady R, Sharma KK. Identification and properties of anti-chaperone-like peptides derived from oxidized bovine lens betaL-crystallins. *J Biol Chem* 2002; 277:39136-43. [PMID: 12176982].
  27. Kannan R, Santhosh kumar P, Mooney BP, Sharma KK.  $\alpha$ A66-80 Peptide interacts with soluble  $\alpha$ -crystallin and induces its aggregation and precipitation: A contribution to age-related cataract formation. *Biochemistry* 2013; 52:3638-50. [PMID: 23631441].
  28. Srivastava OP. Age-related increase in concentration and aggregation of degraded polypeptides in human lenses. *Exp Eye Res* 1988; 47:525-43. [PMID: 3181333].
  29. Harrington V, Srivastava OP, Kirk M. Proteomic analysis of water insoluble proteins from normal and cataractous human lenses. *Mol Vis* 2007; 13:1680-94. [PMID: 17893670].
  30. Chaves JM, Srivastava K, Gupta R, Srivastava OP. Structural and functional roles of deamidation and/or truncation of N- or C-Termini in Human  $\alpha$ A-crystallin. *Biochemistry* 2008; 47:10069-83. [PMID: 18754677].
  31. Asomugha CO, Gupta R, Srivastava OP. Structural and functional roles of deamidation of N146 and/or truncation of NH<sub>2</sub>- or COOH-termini in human  $\alpha$ B-crystallin. *Mol Vis* 2011; 17:2407-20. [PMID: 21976952].
  32. Srivastava OP, Srivastava K. Characterization of three isoforms of a 9 kDa  $\gamma$ D- crystallin fragment isolated from human lenses. *Exp Eye Res* 1996; 62:593-604. [PMID: 8983941].
  33. Srivastava OP, Srivastava K. Cross-linking of human lens 9 kDa  $\gamma$ D-crystallin fragment *in vitro* and *in vivo*. *Mol Vis* 2003; 9:644. [PMID: 14685148].
  34. Rodriguez Plaza JG, Morales-Nava R, Diener C, Schreiber G, Gonzalez ZD, Lara Ortiz MT, Blake IO, Pantoja O, Volkmer R, Klipp E, Herrmann A, Del Rio G. Cell penetrating peptides and cationic antibacterial peptides: Two sides of the same coin. *J Biol Chem* 2014; 289:14448-57. [PMID: 24706763].
  35. Koren E, Torchilin VP. Cell-penetrating peptides: breaking through to the other side. *Trends Mol Med* 2012; 18:385-93. [PMID: 22682515].
  36. Mitchell DJ, Kim DT, Steinman L, Fathman CG, Rothbard JB. Polyarginine enters cells more efficiently than other polycationic homopolymers. *J Pept Res* 2000; 56:318-25. [PMID: 11095185].
  37. Bechara C, Sagan S. Cell-penetrating peptides: 20 years later, where do we stand? *FEBS Lett* 2013; 587:1693-702. [PMID: 23669356].
  38. Srivastava OP, Srivastava K. Existence of deamidated  $\alpha$ B-crystallin fragments in normal and cataractous human lenses. *Mol Vis* 2003; 9:110-8. [PMID: 12707643].
  39. Laemmli UK. Cleavage of structural proteins during the assembly of the head of bacteriophage T4. *Nature* 1970; 227:680-68. [PMID: 5432063].
  40. Gupta R, Srivastava OP. Effect of deamidation of Asparagine 146 modulates functional and structural properties of human lens  $\alpha$ B-crystallin. *Invest Ophthalmol Vis Sci* 2004; 45:206-14. [PMID: 14691175].
  41. Gupta R, Srivastava OP. Deamidation affects structural and functional properties of  $\alpha$ A-crystallin and its oligomerization with  $\alpha$ B-crystallin. *J Biol Chem* 2004; 43:44258-69. [PMID: 15284238].
  42. Su SP, Lyons B, Friedrich M, McArthur JD, Song X, Xavier D, Truscott RJ, Aquilina JA. Molecular signatures of long-lived proteins: autolytic cleavage adjacent to serine residues. *Aging Cell* 2012; 11:1125-7.
  43. Zhang X, Dudek EJ, Liu B, Ding L, Fernandes AF, Liang JJ, Horwitz J, Taylor A, Shang F. Degradation of C-terminal truncated  $\alpha$ A-crystallins by the ubiquitin-proteasome pathway. *Invest Ophthalmol Vis Sci* 2007; 48:4200-8. [PMID: 17724207].

44. Lyons B, Kwan AH, Truscott RJW. Spontaneous cleavage of proteins at serine and threonine is facilitated by zinc. *Aging Cell* 2016; 15:237-44. [PMID: 26751411].
45. Su SP, McArthur JD, Andrew Aquilina J. Localization of low molecular weight crystallin peptides in the aging human lens using a MALDI mass spectrometry imaging approach. *Exp Eye Res* 2010; 91:97-110. [PMID: 20433829].
46. Christopher KL, Pedler MG, Shieh B, Ammar DA, Petrash JM, Mueller NH. Alpha-crystallin-mediated protection of lens cells against heat and oxidative stress-induced cell death. *Biochim Biophys Acta* 2014; 1843:309-15. [PMID: 24275510].
47. Su S-P, Lyons B, Friedrich MG, McArthur JD, Song X. Molecular signature of long-lived proteins: Autolytic cleavage adjacent to serine residues. *Aging Cell* 2012; 11:1125-7. [PMID: 22805275].
48. Ueda Y, Fukiage C, Shih M, Shearer TR, David LL. Mass measurements of C-terminally truncated  $\alpha$ -crystallins from two-dimensional gels identify Lp82 as a major endopeptidase in rat lens. *Mol Cell Proteomics* 2002; 1:357-65. [PMID: 12118077].
49. Nahomi RB, Wang B, Raghavan CT, Voss O, Doseff A, Santhoshkumar P, Nagaraj RH. Chaperone Peptides of  $\alpha$ -Crystallin inhibit epithelial cell apoptosis, protein insolubilization, and opacification in experimental cataracts. *J Biol Chem* 2013; 288:13022-35. [PMID: 23508955].

Articles are provided courtesy of Emory University and the Zhongshan Ophthalmic Center, Sun Yat-sen University, P.R. China. The print version of this article was created on 6 August 2022. This reflects all typographical corrections and errata to the article through that date. Details of any changes may be found in the online version of the article.